Aalto University

OPEN ACCESS

This is an electronic reprint of the original article.
This reprint may differ from the original in pagination and typographic detail.

Nguyen, Minh Truong Xuan; Nguyen, Kha; Pham, Phuong Thi Thuy; Huynh, Ha Ky Phuong ; Pham, Huy Hoang; Cuong, Chi Vo; Nguyen, Son Truong

High-performance Pd-coated Ni nanowire electrocatalysts for alkaline direct ethanol fuel cells

Published in:
Journal of Electroanalytical Chemistry

DOI:
10.1016/j.jelechem.2021.115180

Published: 01/05/2021

Document Version
Peer-reviewed accepted author manuscript, also known as Final accepted manuscript or Post-print

Published under the following license:
CC BY-NC-ND

Please cite the original version:
Nguyen, M. T. X., Nguyen, K., Pham, P. T. T., Huynh, H. K. P., Pham, H. H., Cuong, C. V., & Nguyen, S. T. (2021). High-performance Pd-coated Ni nanowire electrocatalysts for alkaline direct ethanol fuel cells. *Journal of Electroanalytical Chemistry*, *888*, Article 115180. https://doi.org/10.1016/j.jelechem.2021.115180

This material is protected by copyright and other intellectual property rights, and duplication or sale of all or part of any of the repository collections is not permitted, except that material may be duplicated by you for your research use or educational purposes in electronic or print form. You must obtain permission for any other use. Electronic or print copies may not be offered, whether for sale or otherwise to anyone who is not an authorised user.

Graphical Abstract

High-performance Pd-coated Ni Nanowire Electrocatalysts for Alkaline Direct Ethanol Fuel Cells

Minh Truong Xuan Nguyen[1,3], Minh-Kha Nguyen[1,3,4], Phuong Thi Thuy Pham[5], Ha Ky Phuong Huynh[1,3], Huy Hoang Pham[1,3], Cuong Chi Vo[1,2,3], Son Truong Nguyen [1,2,3,*]

[1]*Faculty of Chemical Engineering, Ho Chi Minh City University of Technology (HCMUT), 268 Ly Thuong Kiet St., Dist. 10, Ho Chi Minh City, Vietnam*

[2]*Research Institute for Sustainable Energy, Ho Chi Minh City University of Technology (HCMUT), 268 Ly Thuong Kiet St., Dist. 10, Ho Chi Minh City, Vietnam*

[3]*Vietnam National University Ho Chi Minh City, Linh Trung Ward, Thu Duc Dist., Ho Chi Minh City, Vietnam*

[4]*Department of Neuroscience and Biomedical Engineering, Aalto University School of Science, P.O. Box 12200, FI-00076 Aalto, Finland*

[5]*Institute of Chemical Technology - Vietnam Academy of Science and Technology, TL29 St., Thanh Loc Ward, Dist. 12, Ho Chi Minh City, Vietnam*

* *Corresponding author: ntson@hcmut.edu.vn*

TOC image

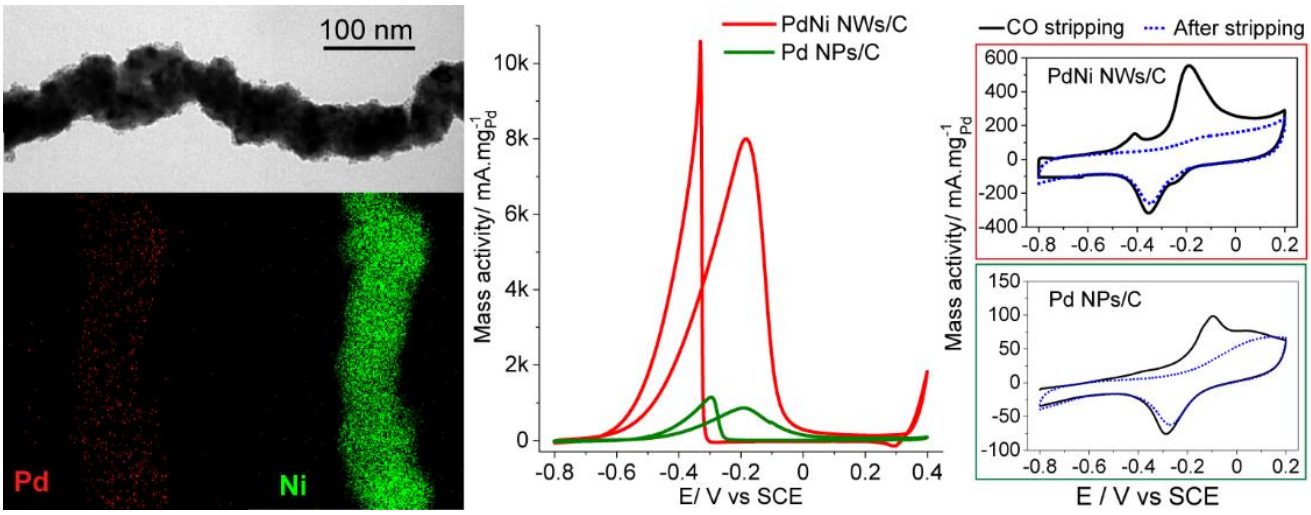

Highlights:

- Pd-coated Ni nanowires (PdNi-NWs/C) with a low Pd:Ni molar ratio were first time prepared.
- A unique Pd coating with a high catalytic efficiency was achieved by controllable synthesized conditions.
- PdNi-NWs/C showed superior catalytic ability in EOR and CO-tolerance compared to palladium nanoparticles (PdNPs/C).
- Remarkable improvement in electro-catalytic activity for EOR derived from the addition of Ni and 1D core-shell structure.

Abstract

The major hindrance for a successful commercialization of direct ethanol fuel cells (DEFCs) is the sluggish ethanol oxidation reaction (EOR) and the rapid poisoning of anodic catalysts by by-products. In this work, a high-performance PdNi nanowire (PdNi-NWs) catalyst was prepared via a two-step process in polyol medium based on the galvanic replacement reaction. By carefully screening parameters for a uniform deposition of Pd layers on Ni nanowires, the PdNi-NWs electrode exhibits a significant enhancement of both catalytic activity and durability for the EOR in alkaline media, which may be ascribed to the electronic structure modification and bifunctional electrocatalytic mechanism with hydroxyl and ethanol bindings on Ni and Pd, respectively. Moreover, these nanowire structures are efficient electron and mass transfer and enriched with abundant active sites by oxygen-rich compounds of Ni. The highest electrocatalytic performance has achieved with a low Pd:Ni molar ratio of 18:100, which reaches 9.3 times superior mass activity and the EOR onset potential shifts 50 mV negatively compared with Pd nanoparticles (PdNPs). These results highlight the active role of PdNi-NWs catalysts in DEFCs.

Keywords: PdNi nanowires, ethanol electrooxidation, bifunctional catalyst, galvanic replacement reaction, CO-like tolerance

1. Introduction

Direct ethanol fuel cells (DEFC) with advantages such as using clean fuel, abundant from biomass sources, high efficiency, large energy density, small design, compact, quiet and operating at low temperatures have been projected to be strong candidates to compete with advanced batteries for powering mobile electronic devices [1, 2]. However, the performance and stability of DEFC in particular and fuel cells in general are facing many barriers and challenges in the commercialization [3, 4]. One of the most important factors influencing on the effectiveness of DEFC is the electrochemical catalysts for the oxidation and reduction processes that take place at anode and cathode, respectively. On the anode, a complete electrooxidation of each ethanol molecule to CO_2 can release 12 electrons ($CH_3CH_2OH + 12OH^- \rightarrow 2CO_2 + 9H_2O + 12e^-$). This pathway requires high activation energy for breaking the C–C bond [5]; hence, there is still distance to achieve a high selectivity of anode catalyst for the direct 12-electron oxidation of ethanol in a fuel cell system. According to the investigations by combining cyclic voltammetry (CV) with NMR spectroscopy and *in-situ* FT-IR spectroscopy [6, 7], the main product of the EOR on all Pd-based anode catalysts in alkaline media is acetate (CH_3COO^-). It is widely accept that the EOR often occurs incompletely through a 4-electron pathway ($C_2H_5OH + 5OH^- \rightarrow CH_3COO^- + 4H_2O + 4e^-$) with state-of-the-art catalysts [5, 8, 9]. The by-product can chemically adsorb and produce a poisoning effect for the EOR in alkaline media on the monometallic Pd catalyst [10-12]. To convert intermediates into more stable forms, one of the given solutions is the combination of Pd and cheaper transition metals (M), e.g., Ag [10, 13], Ni [14-17], Co [2, 18], W [19], resulting not only in improving the efficiency of EOR but also in reducing the amount of Pd precursors. The transition metal can create oxygen-rich compounds with a high oxidation state though its strong affinity with oxygen and accelerate the oxidation of ethanol [8]. Among that, the presence of Ni in PdNi can create a number of oxygen-rich compounds, e.g., NiO, $Ni(OH)_2$ and NiOOH, which promote the EOR [20]. The previous study [21] suggested that Ni^{3+} in NiOOH species

can be as an active site for the direct electro-oxidation of ethanol. With high oxophilicity, Ni can enhance the adsorption of the OH^- group and increase the removal of adsorbed ethoxy intermediates. Calculating the adsorption energy of OH^- on Pd (-214.2 kJ/mol) and on PdNi (-353.2 kJ/mol), Saurav group [22] pointed out that PdNi is a good catalyst for OH^- chemisorption. Additionally, $Ni(OH)_2$, the main component of the Ni species, oxidizes to the oxyhydroxide network via the reversible redox: $Ni(OH)_2 + OH^- \leftrightharpoons NiOOH + H_2O + e^-$, which chiefly accounts for the activation towards EOR on PdNi in alkaline media [23, 24]. Moreover, the transfer of electrons from the less electronegative Ni (1.91) to Pd (2.20) in PdNi structures also lead to down-shift d-band center of Pd. Consequently, the Pd-CO binding energy of CO-like compounds on Pd-based active sites decreases and their adsorptive bonds are weakened, resulting in improvement of CO-tolerance on PdNi [25-27]. Recently, Jelena *et al.* [15] investigated the electrochemical performance of PdNi alloy in EOR and found that $Pd_{0.74}Ni_{0.26}$ can achieve the higher catalytic efficiency than the others. In comparison with pure Pd, $Pd_{0.74}Ni_{0.26}$ showed 3 times higher in current density and 100 mV more negative potential in the onset potential of EOR. These studies make Ni an emerging second metal in effectively combining with Pd to form PdNi bimetallic electrochemical catalyst, which improves the limitations of pure Pd for EOR in alkaline media.

PdNi bimetallic alloy nanospheres are commonly synthesized by the simultaneous reduction of the respective precursors for the oxidation of alcohol [14, 15, 28-30]. However, various investigations on catalytic activity pointed out that only Pd atoms at the surface of the catalyst can provide the active centers for the adsorption and oxidation processes [31]. Consequently, to improve the catalytic performance, most of PdNi alloy structures needs to be synthesized with a rather high Pd:Ni ratio from 0.67:1 to 2.85:1, leading to using a large amount of Pd [14, 15, 26, 32, 33]. Instead of making PdNi alloy, if the bimetallic system is designed as coating Pd on Ni nanoparticles (NPs), it could drastically reduce the amount of Pd precursor, increase the shelf-life of Ni particles, and enhance the catalytic efficiency of Pd layer on the

surface. Besides that, morphologies play critical roles in the performance of the catalysts [34]. Small spherical nanostructures can provide large electrochemical active surfaces, but the large surface energy makes them easy is dissolved and agglomerated into large particles during operation [35]. Meanwhile, the one-dimensional (1D) nanomaterials show several advantages over commonly used small NPs, e.g., good activity and high durability. Due to reduced surface energy, 1D catalysts are able to control dissolution, agglomeration and Ostwald ripening [36]. Furthermore, the 1D structures with few surface boundaries promote the electron transport characteristics, and thereby increase the reaction kinetics on the catalytic surface [37, 38]. Despite these advantages, studies on synthesis and electrocatalytic activity for the EOR of 1D Pd-coated Ni nanostructures have rarely been reported.

Herein, we synthesize the Pd-coated Ni core nanowires (PdNi-NWs) to reduce the Pd loading in the catalyst composition and investigate its anode catalyst performance for DEFC. The Ni nanowires (NiNWs) are first prepared through NPs self-oriented attachment by a polyol method without adding of templates or surfactants. We consider then it worthwhile to investigate whether Pd can be coated over NiNWs by a galvanic replacement reaction in polyol aqueous solution. Screening and optimization studies on the catalytic properties for EOR of PdNi-NWs are observed with varying of synthesis temperature, synthesis time, Pd:Ni precursor ratio and polyvinylpyrrolidone concentration. The uniform nanowires and well Pd coating along with the bifunctional mechanism between Pd and Ni have enhanced significantly the electroactivity and the poisoning tolerance of PdNi-NWs for ethanol electrooxidation.

2. Experimental

2.1. Materials

Nickel (II) chloride hexahydrate ($NiCl_2.6H_2O$, 99%), hydrazine monohydrate ($N_2H_4.H_2O$, 80%), ethylene glycol (EG, 99.5%), polyvinylpyrrolidone (PVP, Mw = 40000), palladium (II) nitrate dehydrate ($Pd(NO_3)_2.2H_2O$ > 99%), Nafion solution (5 wt.% in isopropanol and water),

Al_2O_3 and ethanol (99.5%) were purchased from Sigma Aldrich (Singapore). Vulcan XC-72 carbon black (VC-XC72) was obtained from Cabot Corp. (USA).

2.2. Synthesis of nickel nanowires

Nickel nanowires (NiNWs) were synthesized by a polyol method with N_2H_4 as the reducing agent. Typically, firstly 20 mL of EG and 0.3 g of PVP were added into a three necked flask equipped with a reflux condenser and a thermometer. After that, 0.1 mL of 1 M $NiCl_2$ solution was added into the solution. The mixture was stirred and heated to 100 ^oC, and then N_2H_4 was injected in dropwise. The solution turned black within few seconds. The reaction was operated for 30 min, until the dark grey product appeared and floated on the surface of solution. After being cooled down to room temperature, the sample was diluted with ethanol (at a volume ratio of 1:10), and centrifuged several times at 3000 rpm for 20 min. The obtained product was stored in ethanol for further steps.

2.3. Synthesis of Pd coated NiNWs

Pd coated NiNWs (PdNi-NWs) were synthesized via a galvanic replacement reaction between NiNWs and Pd^{2+} ion in EG. The effect of synthesis temperature, reaction time, Pd:Ni molar ratios and PVP concentration on the nanostructures of PdNi-NWs were investigated. The details are reported in the Supporting Information. For the sample preparation for 180 min at 90 ^oC, NiNWs were dispersed in 10 mL of EG, stirred and heated to 90 ^oC. Then, 2 mL of aqueous $Pd(NO_3)_2$ (with a fixed molar ratio of Pd:Ni at 18:100 based on initial amount of precursor) and PVP (0.1% w/v per 12 mL of the synthesis mixture) were added dropwise for 20 min. Then the solution was stirred for 180 min at 90 ^oC. The obtained product was centrifuged with ethanol and then dried in a vacuum oven for 24 h at 60 ^oC.

2.4. Synthesis of Pd nanoparticles

For comparison, Pd nanoparticles (PdNPs, with average size at 3.5 nm as in Fig. S1) were synthesized based on the process reported in previous research [39] with minor modifications.

Typically, 5 mL of EG was added into a three-neck flask (equipped with a condenser, a thermometer, and a magnetic stirring bar) and heated to 120 ^{o}C. After that, 3 mL deionized water containing 0.0243 g $Pd(NO_3)_2.2H_2O$ and 0.0458 g PVP in 3 mL EG were added into, simultaneously. Followed by, the whole mixture was continually stirred for 60 min. The product was centrifuged and then dried in vacuum oven for 24 h at 60 ^{o}C.

2.5. Catalyst preparation

PdNi-NWs or PdNPs were dispersed on carbon support by mixing with VC-XC72 at a mass ratio of 1:4 to produce catalysts named as PdNi-NWs/C or PdNPs/C. They were stirred in ethanol for 4 h and then dried in vacuum oven at 60 ^{o}C. Finally, the obtained products were preserved for physical and electrochemical investigations.

2.6. Structural characterization

For morphologies investigation, the samples were dispersed in ethanol by ultrasonication, followed by dropping onto copper grids and dried at room temperature. A JEOL 2010 transmission electron microscopy (TEM, 100 keV) was applied to collect TEM images. X-ray powder diffraction was conducted on a D8 Bruker AXS X-ray diffractometer (CuKα radiation, 40 kV, 20 mA). The X-ray photoelectron spectroscopy (XPS) *wide- and narrow*-scan spectra of the sample were obtained by a ThermoScientific K-Alpha photoelectron spectrometer equipped with monochromatic Al K-α ($h\nu$ = 1486.6 eV) at 200 eV pass energy, and 45^{o} take-off angle prior to being curve-fitted by Casa XPS software. All spectra were subtracted using a Shirley background and normalized with the C1s peak set to 284.5 eV, which has been widely assigned for C-C bond in carbon black [40, 41]. An asymmetric modified Lorentzian line shape (LA(1.1,2.2,10)) was employed for fitting metal components while a symmetric Gaussian/Lorentzian one (GL30) was applied for the others. Despite of Ni and Pd valence states, the peak area ratio required for 2p and 3d spin-orbit doublets were constrained to be equal to 2 and 1.5, respectively, while no constraints were applied for the Full Width at Half Maximum (FWHM) and position of all peaks [42].

2.7. Electrochemical investigation

The electrochemical performance of the materials for EOR was carried out by using a Biologic MPG2 potentiostat (France) with a three-electrode cell including glassy carbon electrode (GCE, 4 mm in diameter), Pt mesh and saturated calomel electrode (SCE) as the working, counter and reference electrode, respectively. Cyclic voltammetry (CV), linear sweep voltammetry (LSV) and chronoamperometry (CA) measurements were operated in (1 M KOH + 1 M Ethanol) solution with scan rate of 50 mV/s from -0.8 to 0.2 V vs SCE.

For the preparation of working electrode, alumina slurry was used for polishing GCE at first and then ultrasonically clean with ethanol. The catalyst loading on GCE were prepared by dropping 5 µL of well-dispersed suspension in which 3.3 mg of each catalyst dispersing in 1 mL ethanol by ultrasonication for 1 h. Then 5 µL of 0.5 wt.% Nafion solution in ethanol was applied to fix the catalyst on GCE.

CO stripping test in 1M KOH solution was also employed to investigate the tolerance to CO-like intermediates. CO gas was bubbled into a solution of 1 M KOH while keeping the potential at -0.8 V vs SCE for about 30 min to saturate CO molecules on the catalysts. Then the gas flux was switched from CO to nitrogen for 10 min in order to remove any dissolved CO in solution. For the next step, the CO stripping experiment was proceeded by 10 cycles of CV test with a scan rate of 50 mV/s from -0.8 V to 0.2 V vs SCE at room temperature.

3. Results and discussion

3.1. Influence of synthesis temperature

The templates of PdNi-NWs were prepared by using a synthesized NiNWs with an average diameter and length of 75 nm and 18 µm, respectively (Fig. 1a and S2). Due to a large gap of the standard redox potentials between Pd^{2+}/Pd (+0.915 V) and Ni^{2+}/Ni (-0.25 V), Pd^{2+} ions were reduced by Ni atoms. TEM images shown in Fig. 1 indicate the distinct surfaces between NiNWs and PdNi-NWs prepared at different synthesis temperatures. An operating synthesis system at moderate low temperatures (70 ^{o}C and 80 ^{o}C) forms several PdNPs decorated on

NiNWs' surfaces (Fig. 1b and 1c). Meanwhile, a thin Pd shell layer of small particles can be observed by tuning up to higher temperatures (90 ^{o}C and 100 ^{o}C, Fig. 1d and 1e, respectively). The reasonable explanation is that at low temperatures, the galvanic reaction between Ni and Pd^{2+} may occur with a low rate, thus generated a few PdNPs. This can rise up with an increase of synthesis temperature. As suggesting by Papaderakis group's research [43], a fast galvanic replacement can control the coating into a thin and continuous metallic layer, otherwise a slow replacement resulting in a particulate film. Besides, it is marked that the reaction of Pd^{2+} and EG will occur at a high temperature [39]. As a result, Pd particles not only deposited on NiNWs but also appeared separately outside the templates when increasing temperature to 110^{o}C (Fig. 1f). Therefore, the synthesis temperature plays a crucial role in the diffusion of Pd^{2+} and the coating of Pd(0) on NiNWs' surface during the galvanic replacement reaction in polyol medium.

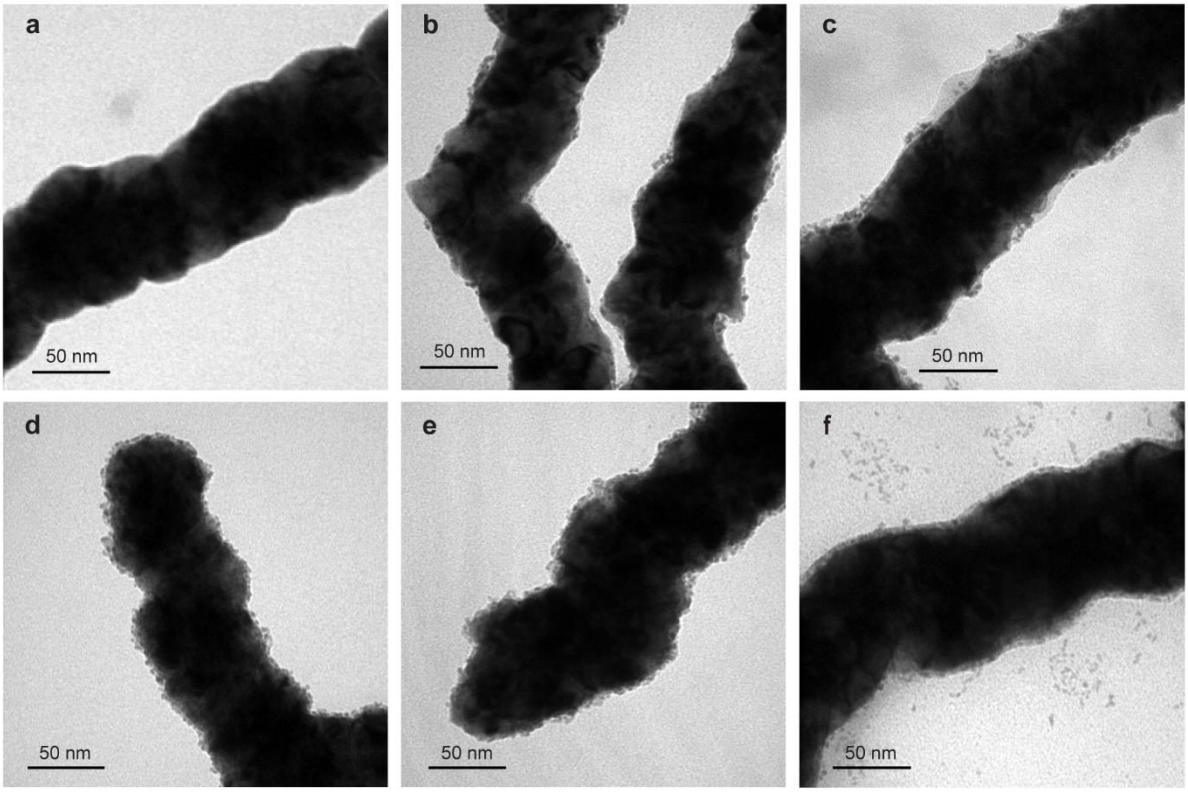

Fig. 1. TEM images of (a) NiNWs and (b-f) PdNi-NWs prepared at different synthesis temperatures. (b) 70 ^{o}C, (c) 80 ^{o}C, (d) 90 ^{o}C, (e) 100 ^{o}C, and (f) 110 ^{o}C.

The PdNi-NWs, which were synthesized at different temperatures and dispersed on VC-XC72, are referred to as PdNi-T*x*/C (*x* is a value of the synthesis temperature). Electro-catalytic performances of PdNi-T*x*/C were analysed to evaluate the difference properties between these samples. Fig. 2a shows CV curves in 1 M KOH solution of NiNWs/C, PdNPs/C and PdNi-T90/C. In the inner image of Fig. 2a, on the forward scanning from -1.0 to -0.5 V, a peak at ca. -0.71 V is typical for the oxidation of Ni(0) to Ni^{2+} [32, 44]. However, this peak disappears on the scanning in the potential range from -0.8 to 0.4 V due to the overlap of a strong peak at ca. 0.33 V which is associated with the further oxidation of Ni^{2+} into a higher oxidation state of nickel, e.g., NiOOH. The reduction of NiOOH compound to Ni^{2+} can be observed at ca. 0.26 V on the backward scanning [45, 46]. Whereas, CV result in Fig. 2a shows a characteristic behaviour of Pd metal in KOH solution that a strong peak at ca. -0.4 V in the backward scanning is attributed to the reduction of PdO into Pd. Hence, the Pd catalytic cites are reactivated for the further oxidation of C_2H_5OH in the next scanning cycles [35, 47-49]. For the PdNi-T90/C sample, the CV curve in Fig. 2a exhibits all the typical peaks of NiNWs/C and PdNPs/C samples. This proves that the synthesized PdNi-NWs material possesses nickel and palladium as major components. The catalytic abilities of PdNi-T*x*/C samples for the electro-oxidation of 1 M C_2H_5OH in 1 M KOH solution were examined with LSV technique in Fig. 2b. The strong redox peak on each LSV curve at ca. -0.3 V is assigned to the electro-oxidation of ethanol in alkaline solution [15, 33]. Their mass activities are in the increasing order: PdNi-T70/C < PdNi-T80/C < PdNi-T110/C < PdNi-T100/C < PdNi-T90. This may be due to the different degrees of Pd coating on NiNWs template under tuning reaction temperature which was analysed by TEM images in Fig. 1. Consequently, preparing catalyst at 90 ^oC can form a rather smooth and unique palladium coating, and create active catalytic sites for improvement of EOR.

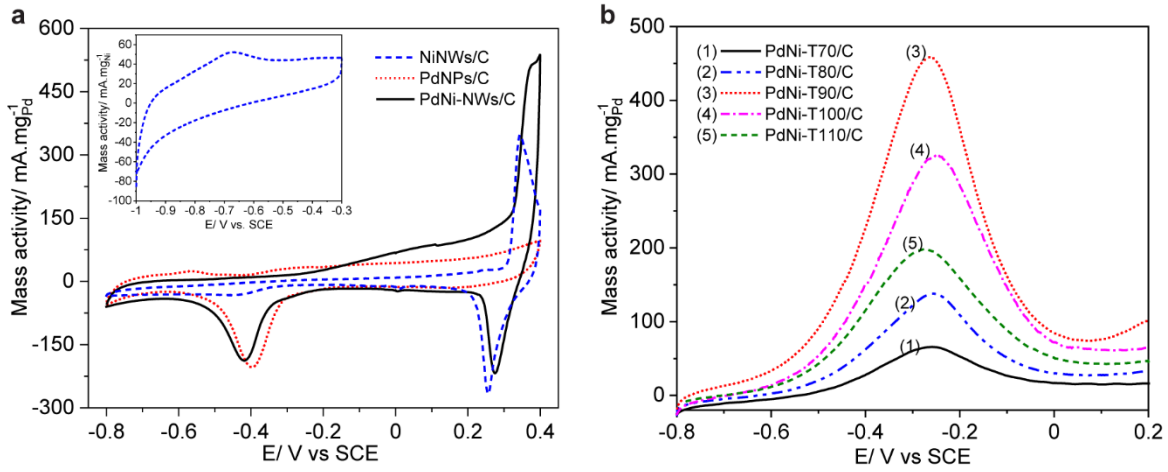

Fig. 2. (a) CV curves of NiNWs/C, PdNPs/C and PdNi-NWs/C in 1M KOH solution and (b) LSV result of the catalysts synthesized at different temperatures in (1 M C_2H_5OH + 1 M KOH) solution with scan rate of 50 mV/s, at room temperature. The inset is CV curve of NiNWs/C with scanning from -1.0 to -0.5 V.

3.2. Influence of synthesis time

PdNi-NWs catalysts synthesized for varying synthesis time and dispersed on Vulcan-XC72 are named as PdNi-*y*min/C, where *y* is the synthesis time. Fig. S3 shows TEM images of the PdNi-*y*min samples prepared for 60 to 210 min, separately. All possess a smooth surface as well as a stable 1D structure after a long duration in the galvanic reaction. Although the difference in morphology between these samples is insignificant, the mass activity of PdNi-*y*min/C arises with an increasing reaction time from 60 to 180 min (Fig. 3). According to the galvanic mechanism reaction [50], lasting reaction time leads to increase the shell coverage degree on the template. As a result, the growth of Pd thickness makes the electro-catalytic efficiency rise. However, a slight reduction is observed in PdNi-210min/C may due to the Pd shell overgrowth suffered from keeping the galvanic reaction longer. This may lead to alter the morphology and thus make the catalytic activity less effective [51] .

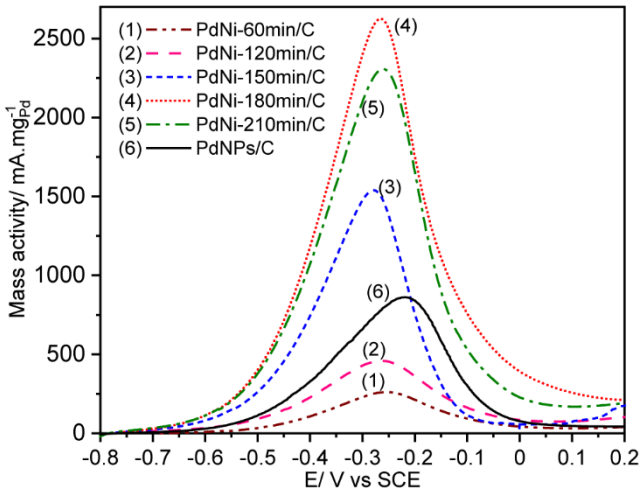

Fig. 3. LSV curves of PdNi-*y*min/C samples prepared for different reaction time in (1 M C_2H_5OH + 1 M KOH) solution with scan rate of 50 mV/s at room temperature.

3.3. Influence of Pd:Ni molar ratio

Varying Pd:Ni molar ratios of relevant precursors from 10:100 to 26:100 were investigated to analyse the influence of Pd:Ni ratio in the formation and growth of PdNPs shell on NiNWs core. The samples are referred to as PdNi-*p:n*, where *p:n* is the molar ratio of Pd:Ni. TEM images in Fig. 4a,b show that a smooth layer of Pd coating on NiNWs was fabricated with the Pd:Ni ratio of 18:100. Remarkably, the coverage of Pd shell became the islands by using the 26:100 ratio. The XRD patterns of NiNWs and PdNi-*p:n* dispersed on carbon support (named as NiNWs/C and PdNi-*p:n*/C, respectively) are presented in Fig. 4c. The strong diffraction peaks at 44.53°, 51.80° and 76.55° are indexed to the (111), (200) and (220) planes, respectively, of a typically crystalline face-centered cubic (fcc) structure of nickel (JCPDS #04-0850, in black). There is an absence of the typical peaks of Pd metal from the XRD patterns. Hence, EDX analysis of the prepared catalyst was applied to identify the elemental composition. The EDX result of PdNi-18:100 sample in Fig. 4d shows that the actual Pd:Ni molar ratio is 15:100. The slight deviation between product and precursor may be due to a loss of Pd in the washing steps and centrifugal. Moreover, high-resolution XPS spectra of PdNi-18:100/C is displayed in Fig. 4e,f. That of the Pd3d core level was well-fitted with six

distinguished peaks by constraining the peak splitting and peak area ratio of Pd3d spin-orbit doublets to be 5.26 eV and 1.5, respectively [42], suggesting the co-existence of at least three different Pd species. However, only the first contribution at 335.7 and 341.0 eV can be undoubtedly assigned to $Pd3d_{5/2}$ and $Pd3d_{3/2}$ characteristic peaks of Pd^0 [41, 52, 53]. The remaining $Pd3d_{5/2}$ peaks at 337.5 and 338.9 eV were assigned to the higher oxidation states $Pd^{\delta+}$ (PdO_x) [54]. The presence of PdO_x could be due to the formation of $Pd(OH)_2$ from the reaction between Pd^{2+} and OH^-, which was generated during the reduction of NO_3^- (in $Pd(NO_3)_2$ precursor) to NO_2^-. After that, $Pd(OH)_2$ dehydrated into PdO_x and deposited on the catalyst's surface [55, 56]. It was noticed that PdO_x thin layer could enhance the adsorption of ethanol and intermediates, leading to promote the catalytic activity for EOR [57]. Nickel has a natural tendency to form a thin layer of NiO, $Ni(OH)_2$ and NiOOH on its surface upon exposure to ambient air [58, 59]. The curve-fitting of the Ni2p XPS spectra is not straightforward due to the emergence of "shake-up" satellite peaks to the main characteristic peaks of the Ni2p core levels [60, 61]. However, the adequate differences in BE between the metallic, oxide and hydroxide species allow qualitative interpretation of XPS spectra of their mixture without exactly taking into account the FWHM and position of the satellite peaks [23, 62, 63]. The $Ni2p_{3/2}$ region that is below 861 eV was fitted with four distinguished peaks at 853.1, 854.8, 856.0, and 857.3 that could be assigned to Ni^0, NiO, $Ni(OH)_2$, and NiOOH [60, 63-68]. The analysis also exhibits that the Pd:Ni atomic ratio on the surface was measured to be 330:100 which is much higher than that of the EDX result (15:100). The result is a markable presence of Pd nanoshell. The difference of Pd:Ni ratio in the product analyzing from XRD, EDX and XPS can be explained that PdNi-18:100/C was prepared by adding a tiny amount of notable palladium to assure its economic feasibility, resulting in no diffraction pattern of palladium in the XRD profiles. The depth for XPS analysis is few nanometers; thus, it was carried out to confirm the occurrence of Pd nanoshell and identify the chemical elements on the surfaces. The results emphasize that our protocol based on the galvanic replacement reaction between Pd^{2+}

ion and NiNWs in EG solution is an effective approach for the preparation of Ni-core – Pd-shell nanowires.

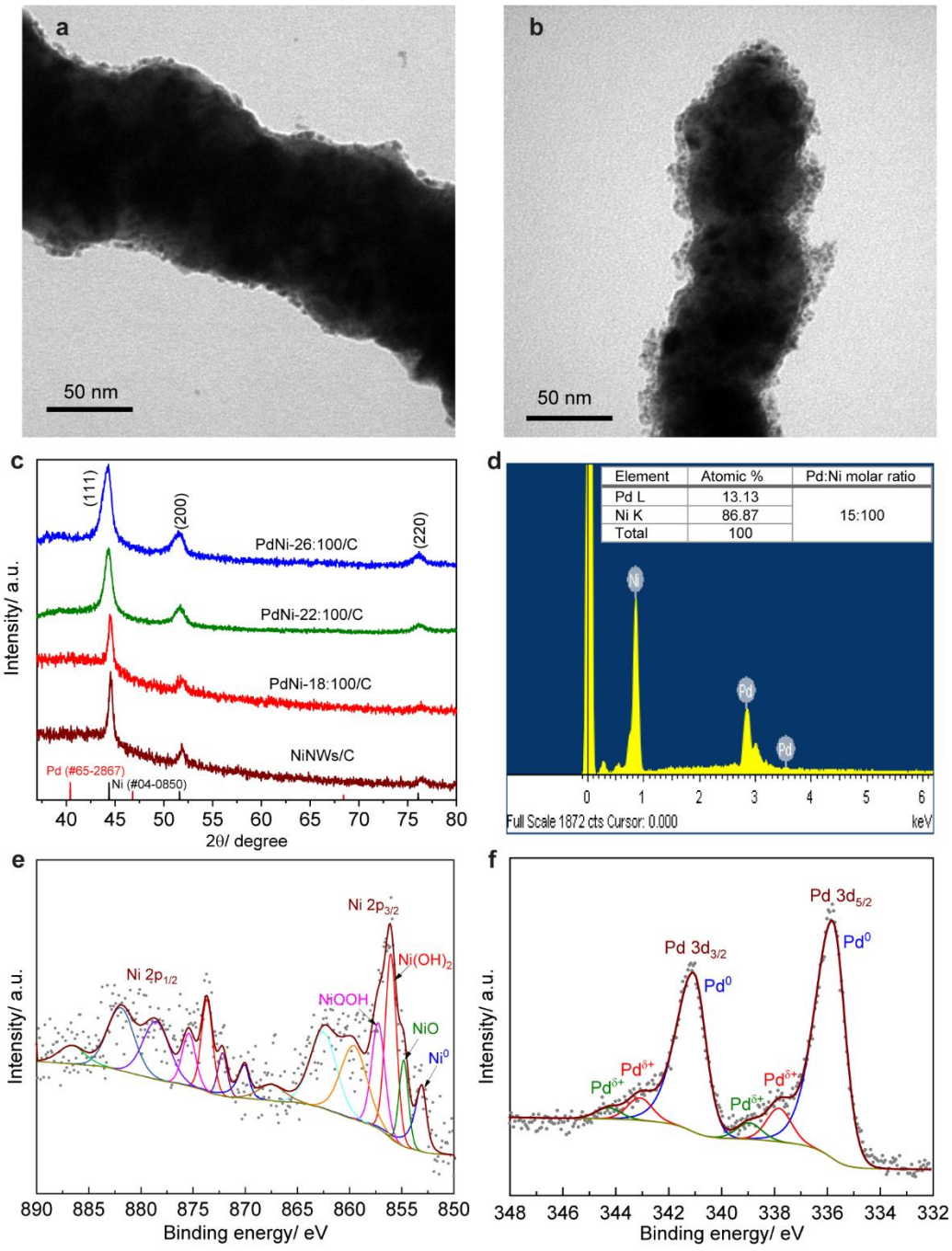

Fig. 4. TEM images of PdNi-18:100 (a) and PdNi-26:100 (b); XRD patterns of PdNi-NWs/C prepared with various Pd:Ni molar ratios (c); EDX spectrum (d), high-resolution XPS spectra at Ni2p (e) and Pd3d (f) core levels of PdNi-18:100/C sample.

The electrocatalytic EOR activities of PdNi-*p:n*/C samples and of PdNPs/C are shown in Fig. 5a. The LSV curves present the catalytic capacities in the following order: PdNPs/C <

PdNi-10:100/C < PdNi-14:100/C < PdNi-26:100/C < PdNi-22:100/C < PdNi-18:100/C. The PdNi-18:100/C sample showed the highest mass activity (4288 $mA.mg_{Pd}^{-1}$) and the most negative onset potential -0.63 V). The increase in Pd:Ni ratios higher than 18:100 leading to decrease in current may be due to nickel atoms exposed on catalyst's surface were completely covered by a thick Pd shell (as can be seen in TEM image of PdNi-26:100, Fig. 4b). Previous researches [33, 46, 69] reported that nickel in bifunctional PdNi catalyst plays an important role in accelerating the overall rate of EOR. The oxophilic Ni promoters generate oxygen-rich species that can support the adsorption of ethanol and OH^- as well as the kinetic process of EOR on the catalytic surface. Besides, XPS of Ni in Fig. 4e also confirms that there are high oxidation state compounds of nickel such as NiO, $Ni(OH)_2$ and NiOOH on the surface of PdNi. Hamdan group [70] suggested that when NiOOH is formed, the adsorption of ethanol on the electrode surface occurs immediately. To further investigate, CV tests of PdNi-*p:n*/C, NiNWs/C and PdNPs/C were carried out in 1 M KOH and (1 M C_2H_5OH + 1 M KOH) solution. In Fig. S4, CV curve of NiNWs/C in 1 M KOH solution demonstrates two oxidation - reduction relative peaks of the $Ni(OH)_2$ and NiOOH (denoted as A_1 and C_1, respectively). In the presence of ethanol (red curve in Fig. S4), the oxidation peak A_1 at ca. 0.3 V of $Ni(OH)_2$ into NiOOH was overlapped with the region A_2 from 0.3 to 0.4 V, which is ascribed to the immediate strong adsorption and oxidation of ethanol after completing the formation of NiOOH [70]. In order to evaluate the contribution of NiOOH in EOR efficient, the CV measurements of PdNi-18:100/C in (1 M C_2H_5OH + 1 M KOH) solution were performed in the various potential ranges from -0.8 to 0.2 V (Fig. S5) and from -0.8 to 0.4 V (Fig. 5b). As seen in Fig. 5b, similarly to the processes on PdNPs/C, the ethanol oxidation reaction on PdNi-18:100/C starts at -0.7 V and a oxidation peak (denoted as A_0) is observed during the forward scan in the potential range between -0.8 and 0.2 V. Remarkably, the addition of Ni in PdNi-NWs catalysts provides the strong oxidation - reduction peaks in the potential range from 0.2 to 0.4 V at C_1 peak and A_2 region while they disappear in the case of PdNPs/C (Fig. 5b). Moreover, the results in Fig. S5

show clearly that the mass activity (I_f) and I_f/I_b ratio achieved in the potential range between -0.8 and 0.4 V are larger than in the range from -0.8 to 0.2 V. The high oxidation state Ni^{3+} in NiOOH is suggested as an active site for the oxidation of ethanol and intermediate as in Eq. 1 and Eq. 2 [21, 71]. This proves the role of NiOOH forming at ca. 0.3 V in the promotion of ethanol adsorption and electro-oxidation.

Ni^{3+} –ethanol → Ni^{3+}–intermediate + e (Eq. 1)

Ni^{3+} –intermediate → Ni^{3+}–product + e (Eq. 2)

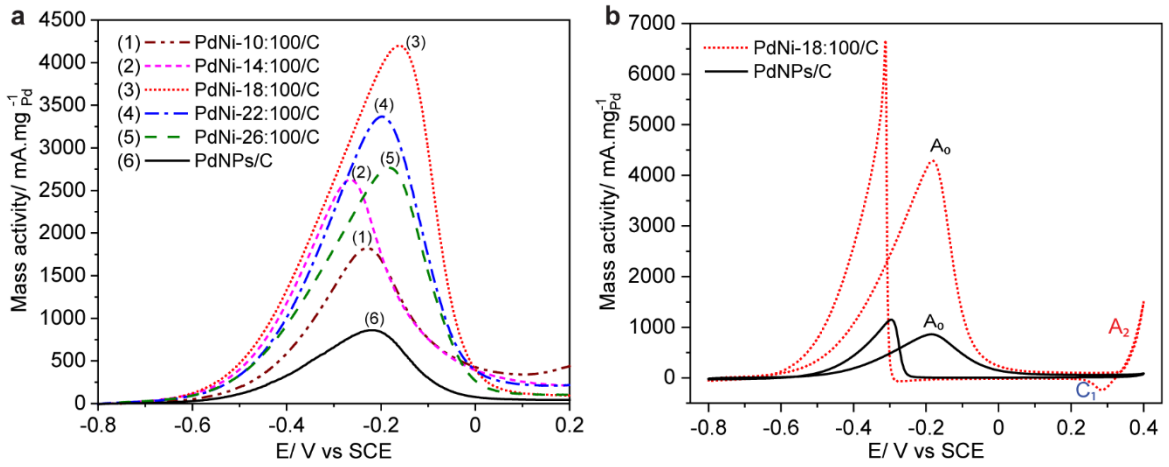

Fig. 5. LSV curves (a) of PdNi-*p:n*/C samples and CV curves (b) of PdNi-18:100/C and PdNPs/C in (1 M C_2H_5OH + 1 M KOH) solution at room temperature with scan rate at 50 mV/s.

3.4. Influence of PVP concentration

To examine the influence of a capping agent on the core-shell structure of PdNi-NWs, PVP concentration was increased from 0 to 0.5% w/v in the synthesis procedure. The samples are named as PdNi-zPVP, where *z* is the concentration (% w/v) of PVP. TEM images in Fig. 6a-f show clearly that Pd nanoclusters agglomerated into large particles and formed a uniform coating layer on NiNWs' surface when using a PVP concentration lower than 0.1% w/v and in the range from 0.1% to 0.5% w/v, respectively. It is known that a PdNi synthesis without or with a low PVP is insufficient protecting of Pd nuclei, hence the further growth of Pd layer on

these nuclei develops with different orients [72]. To characterize the distribution of Ni and Pd on the core-shell PdNi-NWs, the EDS elemental mapping analysis was applied for PdNi-0.1PVP sample. As shown in Fig. 6g-i, Ni-core nanowire is coated uniformly by Pd-shell. It confirmed that PVP is an effective surfactant for compensating the high surface energy of PdNPs and controlling them into a smooth shell.

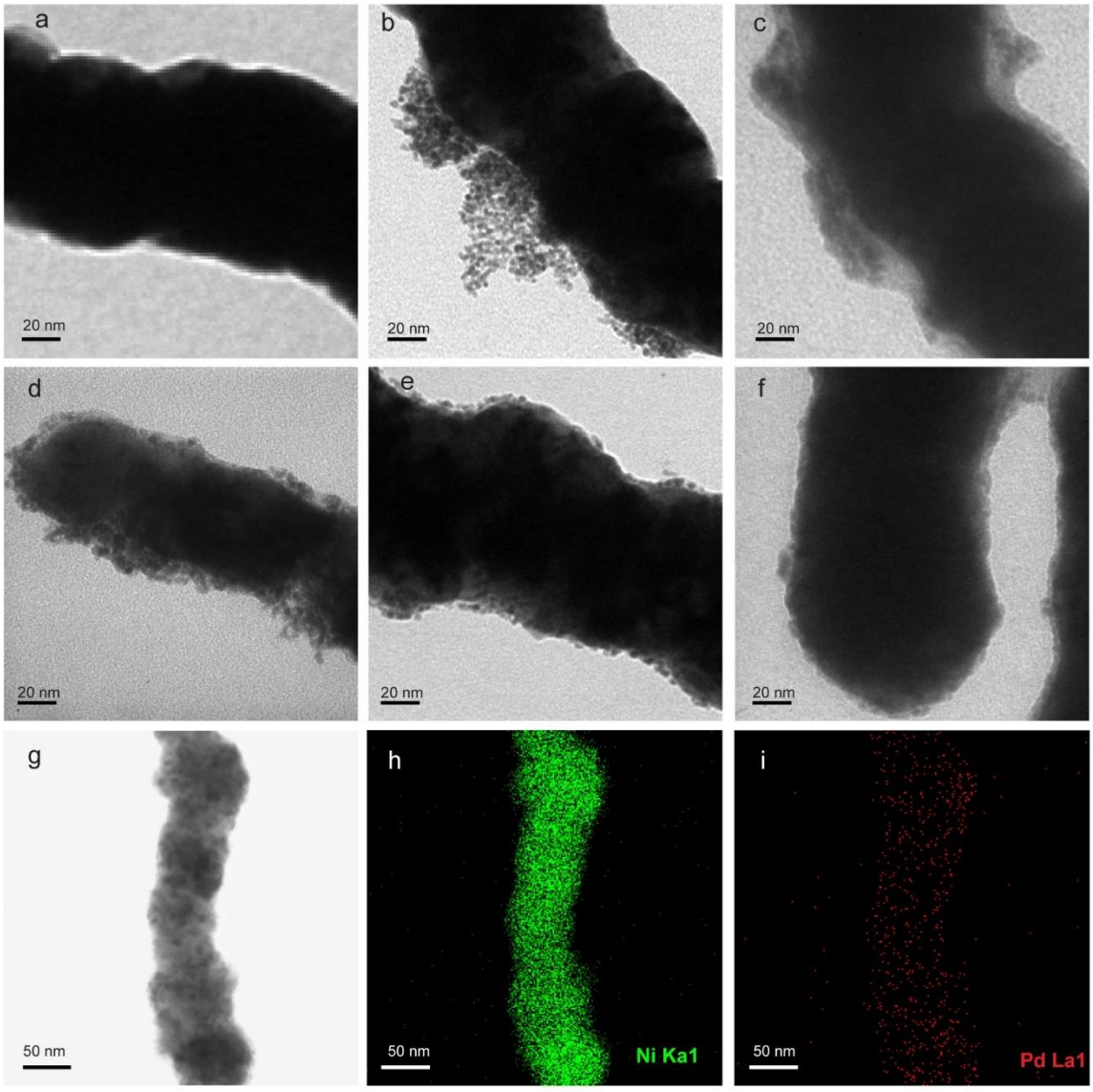

Fig. 6. TEM images of NiNWs (a), PdNi-NWs synthesized without PVP (b), and in the presence of (c) 0.05% w/v, (d) 0.1% w/v, (e) 0.3% w/v, (f) 0.5% w/v PVP. HAADF-STEM image (g), and EDS elemental mapping for Ni (h) and Pd (i) of PdNi-0.1PVP sample.

The LSV curves of PdNi-zPVP samples in (1 M KOH + 1 M C_2H_5OH) solution are shown in Fig. 7a. The results show that PdNi-0.1PVP sample exhibits the highest mass activity (7999

$mA.mg_{Pd}^{-1}$) and the most negative onset potential (-0.64 V) for EOR. Due to the agglomeration of Pd into large particles on PdNi-NWs' surface when using a PVP concentration lower than 0.1% w/v (as shown in Fig. 6b,c), the number of active Pd sites significantly reduce, hence, the mass activity of these samples is much lower than of others (Fig. 7a). Meanwhile, the mass activity down to 4288 and 2093 $mA.mg_{Pd}^{-1}$ after increasing PVP concentration (w/v) to 0.3% and 0.5%. For stabilization, Han et al. [24] investigated the property of C=O group in PVP when it interacts with PdNPs (denoted as PVP-Pd) and in pristine PVP molecules by analyzing FT-IR spectra. They pointed out that peak of C=O in PVP-Pd shifted to a lower wave number (1636 cm^{-1}) compared to pristine PVP (1655 cm^{-1}), proving the occurred coordination of C=O group to PdNPs. Hence, the interaction of PdNi-NWs' surface with a high density of PVP molecules may lock the active catalytic sites; therefore, it limits even hinders the adsorption of ethanol molecules and hydroxyl groups. Consequently, the catalytic ability has been significantly reduced when the concentration of PVP higher than 0.1% w/v.

Moreover, the total electrochemical resistance and activation energy of ethanol electro-oxidation reactions over the catalysts also contribute to the elucidation of the catalytic activities. Here, the charge transfer resistances of PdNi-zPVP/C catalysts was analyzed by the electrochemical impedance spectroscopy (EIS). Nyquist plots of EIS in Fig. 7b indicate that their charge transfer resistances are in the increasing order: PdNi-0.1PVP/C < PdNi-0.3PVP/C < PdNi-0.5PVP/C < PdNPs/C. It means that PdNi-NWs exhibit a faster electron exchange at the electrode/electrolyte interface than Pd nanospheres. Besides, the activation energy of EOR (E_a) can be determined according to Arrhenius equation [13] as in Eq. 3:

$$\ln I = \ln A - E_a / (RT) \qquad \text{(Eq. 3)}$$

where I is the current at a certain potential, R is the ideal gas constant, T is specific temperature and E_a is the activation energy. For calculation of E_a, CV results in Fig. S6a,c of PdNi-0.1PVP/C and PdNPs/C samples were analyzed by plotting currents at ca. -0.2 V as a function of the logarithm of each corresponding testing temperature. As shown in Fig. S6b,d, good linear

responses were achieved in the temperature range from 20 to 60 °C, spanning the range of temperatures commonly found in DEFCs. These fitting data presented that E_a of EOR on PdNi -0.1PVP/C and PdNPs/C are 12.54 and 19.52 kJ /mol, respectively. As a result, the mass activity and onset potential of PdNi-0.1PVP/C sample are 9.3 times greater and 50 mV more negative, respectively, in comparison with PdNPs/C toward EOR (Table S2 and Fig. S7).

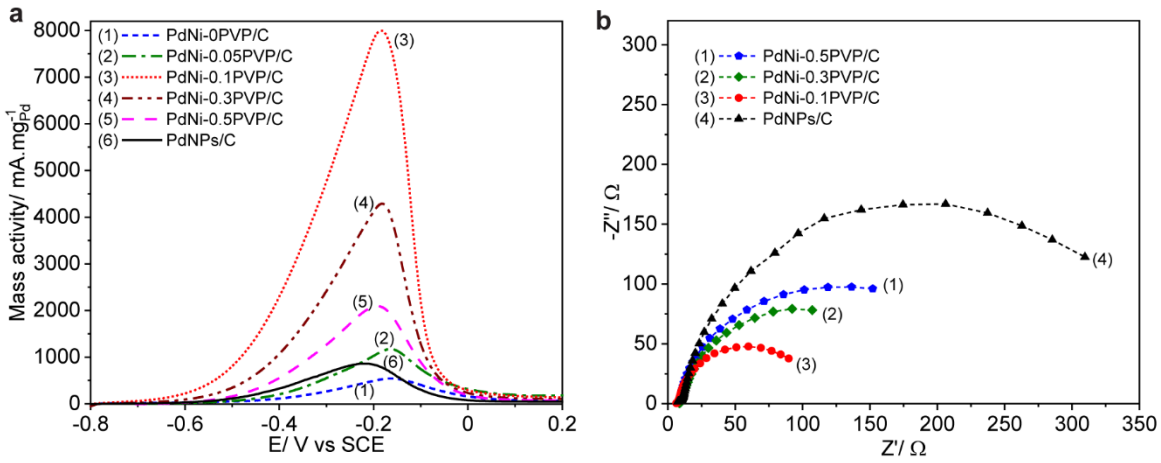

Fig. 7. (a) LSV curves and (b) Nyquist plots of Pd/C and PdNi-zPVP/C catalysts at −0.3 V in (1 M KOH + 1 M C_2H_5OH) solution at room temperature with scan rate at 50 mV/s.

3.5. Electrochemical durability and CO poisoning tolerance of catalysts

The chronoamperometric (CA) in solution (1 M C_2H_5OH + 1 M KOH) at -0.42 V vs SCE was applied to investigate the durability of catalysts. CA test for 3600 s in Fig. 8a shows that in the early stages, high mass activities of two samples were produced due to the rapid oxidation of ethanol. After an adsorption of CO-like intermediates, they both decrease significantly in the first 100 s and decay slow down at further times [33, 73]. After 3600 s, PdNi-0.1PVP/C sample still maintains a higher activity than PdNPs/C.

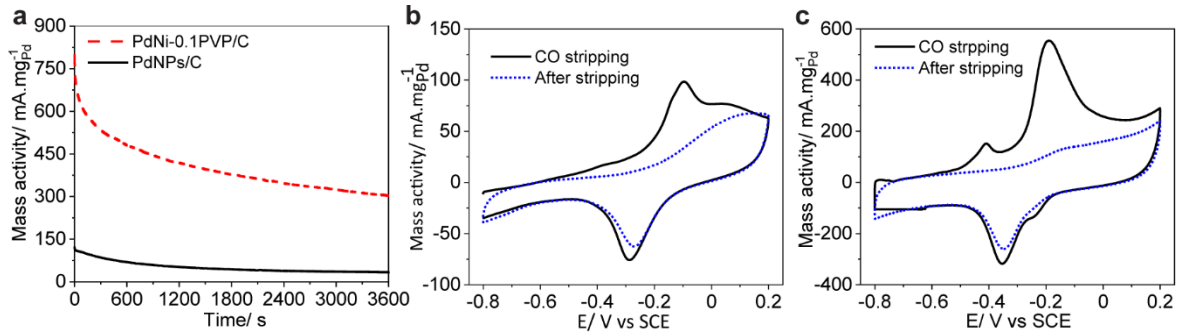

Fig. 8. CA results in (1 M C_2H_5OH + 1 M KOH) solution (a) and CO stripping voltammograms in 1 M KOH at 25 ◦C and scan rate of 50 mV/s of PdNPs/C (b) and PdNi-0.1PVP/C (c).

The tolerance to CO-like intermediates formed during the EOR of PdNi-0.1PVP/C and PdNPs/C are shown in Fig. 8b,c. It can be observed on the forward scan that PdNi-NWs shows two strong peaks at -0.41 V and -0.20 V (with the corresponded onset potentials at -0.50 V and -0.27 V, respectively), but there is only a strong peak at -0.15 V along with the onset potential at -0.24 V on PdNPs/C sample. The peaks at higher potential (-0.15 V and -0.20 V) of two samples are related to the oxidation of CO molecules on isolated Pd sites [49, 74]. Meanwhile, the peak at lower potential of PdNi-0.1PVP/C can be attributed to CO electro-oxidation on PdNi phase produced from the galvanic reaction between Pd^{2+} ions and Ni atoms, agreeing with previous reports [75]. This result shows that the oxidation of CO on PdNi-NWs occurs earlier than on monometallic Pd. The reasonable explanation is that combining Pd with a less electronegative metal such as Ni can lead the transfer of electron from Ni to Pd that is lower the Pd-CO binding energy. Consequently, the adsorptive bonds between CO molecules and Pd catalytic sites are weakened which can help the oxidation of CO easier [25, 76, 77]. Besides that, adding the transition Ni metal into Pd-based nanostructures can promote oxygen-rich species with a high oxophilicity surface [8]. This behaviour can enhance not only the adsorption of the OH^- group but also of ethanol molecules on PdNi catalyst in alkaline media and increase the removal of adsorbed ethoxy intermediates and the overall rate of EOR. As a result, the negative shift of the CO oxidation peak in PdNi-NWs/C was observed, proving that PdNi catalyst possesses a tolerance to CO-like intermediates more than pure Pd.

Additionally, electro-catalytic properties of PdNi catalyst for EOR in alkaline medium of other relevant works are also collected and summarized in Table 1. The data demonstrate that a combination of Pd and Ni in the synthesis of core-shell nanostructures catalyst not only help to minimize the quantity of Pd precursor but also enhance the electrocatalytic efficient. Moreover, the 1D structures with less surface boundaries can help the PdNi-NWs catalyst prevent from Ostward ripening effect during the galvanic process [78] as well as during the EOR catalytic working [31, 36, 39, 48, 79]. Therefore, PdNi-0.1PVP/C exhibits a higher EOR activity and stronger poisoning tolerance not only than as-prepared and pure PdNPs samples in this study but also other PdNi catalysts in previous reports as shown in Table 1. The results make PdNi-NWs core-shell a promising as well as competitive candidates for anodic catalysts in alkaline DEFCs.

Table 1. The EOR electrochemical properties of several relevant PdNi-based catalysts

Materials	Pd:Ni atomic ratio	EOR onset potential	Mass activity (mA/mg_{Pd})	Ref.
PdNi-01.PVP/C (Nanowires, core Ni - shell Pd)	18:100	-0.64 V vs SCE	7999	This research
PdNPs/C (Pd nanospheres)	--	-0.59 V vs SCE	861	This research
PdNPs/C	--	--	880.5	[20]
Commercial Pd/C	--	--	827	[80]
PdNi/C	1: 1.12 (~ 89:100)	0.4 V vs RHE (-0.67 V vs SCE)	2300	[26]

Pd_2Ni_1/C	2:1 (200:100)	--	2956	[46]
PdNi	~ 80:100	-0.6 V vs SCE	--	[73]

4. Conclusions

Pd coated NiNWs with a low Pd content has been successfully synthesized in polyol medium based on galvanic reaction for the first time. The synthetic factors including temperature, reaction time, molar ratio of Pd:Ni and PVP concentration have strongly affected on the formation of a Pd coating on NiNWs' surfaces as well as their electro-catalytic performance for EOR. The efficiency in EOR was gradual increased with the increase of synthesis temperature from 70 to 90 °C. Meanwhile, along with the increasing of synthesis time from 60 to 180 min, the catalytic activity increased gradually and tended to decrease with longer synthesis duration. Besides, the study also showed that the highest catalytic efficiency of PdNi can be achieved when combining Pd with Ni at Pd:Ni ratio of 18:100 in the presence of 0.1% PVP. Higher than 0.1% leads to lock Pd active sites while lower than 0.1% limits the unique Pd coating depositing on nickel wire surface. When compared with pure Pd, the electrochemical oxidation of ethanol occurred on PdNi was much more efficient and its durability over time as well as the ability of CO – tolerance were also superior.

Acknowledgement

The authors are very grateful to Vietnam National Foundation for Science and Technology Development - NAFOSTED for financial support through the project code 104.05-2017.34 and the support of time and facilities from Ho Chi Minh City University of Technology (HCMUT), VNU-HCM for this study and Mr. Khoa Dang Vu for his assistance in CV measurement.

References

[1] Y. Zhang, F. Gao, C. Wang, Y. Shiraishi, Y. Du, Engineering Spiny PtFePd@PtFe/Pt Core@Multishell Nanowires with Enhanced Performance for Alcohol Electrooxidation, ACS Applied Materials & Interfaces 11(34) (2019) 30880-30886.

[2] C. Li, Q. Yuan, B. Ni, T. He, S. Zhang, Y. Long, L. Gu, X. Wang, Dendritic defect-rich palladium-copper-cobalt nanoalloys as robust multifunctional non-platinum electrocatalysts for fuel cells, Nat Commun 9(1) (2018) 3702.

[3] X. Yu, S. Ye, Recent advances in activity and durability enhancement of Pt/C catalytic cathode in PEMFC, Journal of Power Sources 172(1) (2007) 133-144.

[4] Z.Q. Tian, S.P. Jiang, Y.M. Liang, P.K. Shen, Synthesis and Characterization of Platinum Catalysts on Multiwalled Carbon Nanotubes by Intermittent Microwave Irradiation for Fuel Cell Applications, The Journal of Physical Chemistry B 110(11) (2006) 5343-5350.

[5] L. An, T.S. Zhao, Y.S. Li, Carbon-neutral sustainable energy technology: Direct ethanol fuel cells, Renewable and Sustainable Energy Reviews 50 (2015) 1462-1468.

[6] X. Fang, L. Wang, P.K. Shen, G. Cui, C. Bianchini, An in situ Fourier transform infrared spectroelectrochemical study on ethanol electrooxidation on Pd in alkaline solution, Journal of Power Sources 195(5) (2010) 1375-1378.

[7] Z.-Y. Zhou, Q. Wang, J.-L. Lin, N. Tian, S.-G. Sun, In situ FTIR spectroscopic studies of electrooxidation of ethanol on Pd electrode in alkaline media, Electrochimica Acta 55(27) (2010) 7995-7999.

[8] E.A. Monyoncho, T.K. Woo, E.A. Baranova, Ethanol electrooxidation reaction in alkaline media for direct ethanol fuel cells, Electrochemistry: Volume 15, The Royal Society of Chemistry2019, pp. 1-57.

[9] C. Bianchini, P.K. Shen, Palladium-Based Electrocatalysts for Alcohol Oxidation in Half Cells and in Direct Alcohol Fuel Cells, Chemical Reviews 109(9) (2009) 4183-4206.

[10] H. Lv, L. Sun, A. Lopes, D. Xu, B. Liu, Insights into Compositional and Structural Effects of Bimetallic Hollow Mesoporous Nanospheres toward Ethanol Oxidation Electrocatalysis, J Phys Chem Lett 10(18) (2019) 5490-5498.

[11] Z.-R. Yang, S.-Q. Wang, J. Wang, A.-J. Zhou, C.-W. Xu, Pd supported on carbon containing nickel, nitrogen and sulfur for ethanol electrooxidation, Scientific Reports 7(1) (2017) 15479.

[12] R. Pattabiraman, Electrochemical investigations on carbon supported palladium catalysts, Applied Catalysis A: General 153(1) (1997) 9-20.

[13] C. Peng, Y. Hu, M. Liu, Y. Zheng, Hollow raspberry-like PdAg alloy nanospheres: High electrocatalytic activity for ethanol oxidation in alkaline media, Journal of Power Sources 278 (2015) 69-75.

[14] J. Torrero, M. Montiel, M.A. Peña, P. Ocón, S. Rojas, Insights on the electrooxidation of ethanol with Pd-based catalysts in alkaline electrolyte, International Journal of Hydrogen Energy 44(60) (2019) 31995-32002.

[15] J.D. Lović, V. Jović, Electrochemical behavior of electrodeposited Pd and PdNi coatings for the ethanol oxidation reaction in alkaline solution, Journal of Electrochemical Science and Engineering 8(1) (2018) 39-47.

[16] Y. Xiong, Q.L. Liu, A.M. Zhu, S.M. Huang, Q.H. Zeng, Performance of organic–inorganic hybrid anion-exchange membranes for alkaline direct methanol fuel cells, Journal of Power Sources 186(2) (2009) 328-333.

[17] V. Bambagioni, C. Bianchini, J. Filippi, W. Oberhauser, A. Marchionni, F. Vizza, R. Psaro, L. Sordelli, M.L. Foresti, M. Innocenti, Ethanol oxidation on electrocatalysts obtained by spontaneous deposition of palladium onto nickel-zinc materials, ChemSusChem 2(1) (2009) 99-112.

[18] L.A. Fard, R. Ojani, J.B. Raoof, E.N. Zare, M.M. Lakouraj, PdCo porous nanostructures decorated on polypyrrole @ MWCNTs conductive nanocomposite—Modified glassy carbon

electrode as a powerful catalyst for ethanol electrooxidation, Applied Surface Science 401 (2017) 40-48.

[19] Y. Yang, M. Tian, Q. Li, Y. Min, Q. Xu, S. Chen, Ethanol Electrooxidation Catalyzed by Tungsten Core@Palladium Shell Nanoparticles, ACS Appl Mater Interfaces 11(34) (2019) 30968-30976.

[20] Y. Feng, D. Bin, B. Yan, Y. Du, T. Majima, W. Zhou, Porous bimetallic PdNi catalyst with high electrocatalytic activity for ethanol electrooxidation, J Colloid Interface Sci 493 (2017) 190-197.

[21] N. Bahrami Panah, I. Danaee, M. Payehghadr, A. Madahi, Effect of Copper Alloying on Electro-Catalytic Activity of Nickel for Ethanol Oxidation in Alkaline Media, Acta Chim Slov 65(2) (2018) 312-318.

[22] S.C. Sarma, U. Subbarao, Y. Khulbe, R. Jana, S.C. Peter, Are we underrating rare earths as an electrocatalyst? The effect of their substitution in palladium nanoparticles enhances the activity towards ethanol oxidation reaction, Journal of Materials Chemistry A 5(44) (2017) 23369-23381.

[23] S. Shen, T. Zhao, J. Xu, Y. Li, Synthesis of PdNi catalysts for the oxidation of ethanol in alkaline direct ethanol fuel cells, Journal of Power Sources 195(4) (2010) 1001-1006.

[24] S.A. Elsherif, E.N. El Sawy, N.A. Abdel Ghany, Polyol synthesized graphene/PtxNi100-x nanoparticles alloy for improved electrocatalytic oxidation of methanol in acidic and basic media, Journal of Electroanalytical Chemistry 856 (2020) 113601.

[25] Y.L. Qin, J. Wang, F.Z. Meng, L.M. Wang, X.B. Zhang, Efficient PdNi and PdNi@Pd-catalyzed hydrogen generation via formic acid decomposition at room temperature, Chem Commun (Camb) 49(85) (2013) 10028-30.

[26] H. Yang, H. Wang, H. Li, S. Ji, M.W. Davids, R. Wang, Effect of stabilizers on the synthesis of palladium–nickel nanoparticles supported on carbon for ethanol oxidation in alkaline medium, J. Power Sources 260 (2014) 12-18.

[27] A.F.B. Barbosa, V.L. Oliveira, J. van Drunen, G. Tremiliosi-Filho, Ethanol electro-oxidation reaction using a polycrystalline nickel electrode in alkaline media: Temperature influence and reaction mechanism, Journal of Electroanalytical Chemistry 746 (2015) 31-38.

[28] L. Chen, L. Lu, H. Zhu, Y. Chen, Y. Huang, Y. Li, L. Wang, Improved ethanol electrooxidation performance by shortening Pd–Ni active site distance in Pd–Ni–P nanocatalysts, Nature Communications 8(1) (2017) 14136.

[29] B. Cermenek, B. Genorio, T. Winter, S. Wolf, J.G. Connell, M. Roschger, I. Letofsky-Papst, N. Kienzl, B. Bitschnau, V. Hacker, Alkaline Ethanol Oxidation Reaction on Carbon Supported Ternary PdNiBi Nanocatalyst using Modified Instant Reduction Synthesis Method, Electrocatalysis 11(2) (2020) 203-214.

[30] R.S. Amin, R.M. Abdel Hameed, K.M. El-Khatib, M. Elsayed Youssef, Electrocatalytic activity of nanostructured Ni and Pd–Ni on Vulcan XC-72R carbon black for methanol oxidation in alkaline medium, International Journal of Hydrogen Energy 39(5) (2014) 2026-2041.

[31] T.S. Rodrigues, A.H.M. da Silva, A.G.M. da Silva, D.G. Ceara, J.F. Gomes, J.M. Assaf, P.H.C. Camargo, Hollow AgPt/SiO2 nanomaterials with controlled surface morphologies: is the number of Pt surface atoms imperative to optimize catalytic performances?, Catalysis Science & Technology 6(7) (2016) 2162-2170.

[32] M.D. Obradović, Z.M. Stančić, U.Č. Lačnjevac, V.V. Radmilović, A. Gavrilović-Wohlmuther, V.R. Radmilović, S.L. Gojković, Electrochemical oxidation of ethanol on palladium-nickel nanocatalyst in alkaline media, Applied Catalysis B: Environmental 189 (2016) 110-118.

[33] J.L. Tan, A.M. De Jesus, S.L. Chua, J. Sanetuntikul, S. Shanmugam, B.J.V. Tongol, H. Kim, Preparation and characterization of palladium-nickel on graphene oxide support as anode catalyst for alkaline direct ethanol fuel cell, Applied Catalysis A: General 531 (2017) 29-35.

[34] Z.R. Yang, S.Q. Wang, J. Wang, A.J. Zhou, C.W. Xu, Pd supported on carbon containing nickel, nitrogen and sulfur for ethanol electrooxidation, Sci Rep 7(1) (2017) 15479.

[35] H. Lv, Y. Wang, A. Lopes, D. Xu, B. Liu, Ultrathin PdAg single-crystalline nanowires enhance ethanol oxidation electrocatalysis, Applied Catalysis B: Environmental 249 (2019) 116-125.

[36] J.C. Meier, C. Galeano, I. Katsounaros, J. Witte, H.J. Bongard, A.A. Topalov, C. Baldizzone, S. Mezzavilla, F. Schuth, K.J.J. Mayrhofer, Design criteria for stable Pt/C fuel cell catalysts, Beilstein J Nanotechnol 5 (2014) 44-67.

[37] L. Huang, J. Yang, M. Wu, Z. Shi, Z. Lin, X. Kang, S. Chen, PdAg@Pd core-shell nanotubes: Superior catalytic performance towards electrochemical oxidation of formic acid and methanol, Journal of Power Sources 398 (2018) 201-208.

[38] Y. Zhang, F. Gao, C. Wang, Y. Shiraishi, Y. Du, Engineering Spiny PtFePd@PtFe/Pt Core@Multishell Nanowires with Enhanced Performance for Alcohol Electrooxidation, ACS Appl Mater Interfaces 11(34) (2019) 30880-30886.

[39] R.C. Cerritos, M. Guerra-Balcázar, R.F. Ramírez, J. Ledesma-García, L.G. Arriaga, Morphological Effect of Pd Catalyst on Ethanol Electro-Oxidation Reaction, Materials 5(9) (2012) 1686-1697.

[40] S. Contarini, S. Howlett, C. Rizzo, B.J.A.s.s. De Angelis, XPS study on the dispersion of carbon additives in silicon carbide powders, 51(3-4) (1991) 177-183.

[41] J.C. Bertolini, P. Delichere, B.C. Khanra, J. Massardier, C. Noupa, B. Tardy, Electronic properties of supported Pd aggregates in relation with their reactivity for 1,3-butadiene hydrogenation, Catalysis Letters 6(2) (1990) 215-223.

[42] J. Chastain, R.C.J.P.-E.C. King Jr, Handbook of X-ray photoelectron spectroscopy, 40 (1992) 221.

[43] A. Papaderakis, I. Mintsouli, J. Georgieva, S. Sotiropoulos, Electrocatalysts Prepared by Galvanic Replacement, Catalysts 7(12) (2017).

[44] Š. Trafela, J. Zavašnik, S. Šturm, K.Ž. Rožman, Formation of a Ni(OH)2/NiOOH active redox couple on nickel nanowires for formaldehyde detection in alkaline media, Electrochim. Acta 309 (2019) 346-353.

[45] T. Gunji, F. Matsumoto, Electrocatalytic Activities towards the Electrochemical Oxidation of Formic Acid and Oxygen Reduction Reactions over Bimetallic, Trimetallic and Core–Shell-Structured Pd-Based Materials, Inorganics 7(3) (2019).

[46] Z. Zhang, L. Xin, K. Sun, W. Li, Pd–Ni electrocatalysts for efficient ethanol oxidation reaction in alkaline electrolyte, International Journal of Hydrogen Energy 36(20) (2011) 12686-12697.

[47] Z.X. Liang, T.S. Zhao, J.B. Xu, L.D. Zhu, Mechanism study of the ethanol oxidation reaction on palladium in alkaline media, Electrochimica Acta 54(8) (2009) 2203-2208.

[48] Y.-y. Zhang, Q.-f. Yi, H. Chu, H.-d. Nie, Catalytic activity of Pd-Ag nanoparticles supported on carbon nanotubes for the electro-oxidation of ethanol and propanol, Journal of Fuel Chemistry and Technology 45(4) (2017) 475-483.

[49] J. Zhong, D. Bin, Y. Feng, K. Zhang, J. Wang, C. Wang, J. Guo, P. Yang, Y. Du, Synthesis and high electrocatalytic activity of Au-decorated Pd heterogeneous nanocube catalysts for ethanol electro-oxidation in alkaline media, Catalysis Science & Technology 6(14) (2016) 5397-5404.

[50] S.M. Alia, Y.S. Yan, B.S. Pivovar, Galvanic displacement as a route to highly active and durable extended surface electrocatalysts, Catal. Sci. Technol. 4(10) (2014) 3589-3600.

[51] F. Merkoçi, J. Patarroyo, L. Russo, J. Piella, A. Genç, J. Arbiol, N.G. Bastús, V. Puntes, Understanding galvanic replacement reactions: the case of Pt and Ag, Materials Today Advances 5 (2020) 100037.

[52] F.U. Hillebrecht, J.C. Fuggle, P.A. Bennett, Z. Zołnierek, C.J.P.R.B. Freiburg, Electronic structure of Ni and Pd alloys. II. X-ray photoelectron core-level spectra, 27(4) (1983) 2179.

[53] R.M. Mironenko, O.B. Belskaya, A.V. Lavrenov, V.A. Likholobov, Palladium–Ruthenium Catalyst for Selective Hydrogenation of Furfural to Cyclopentanol, Kinetics and Catalysis 59(3) (2018) 339-346.

[54] A.V. Naumkin, A. Kraut-Vass, S.W. Gaarenstroom, C.J. Powell, NIST X-ray Photoelectron Spectroscopy Database, NIST Standard Reference Database Number 20, National Institute of Standards and Technology (NIST), United States of America, 2012.

[55] T. Yoshida, D. Komatsu, N. Shimokawa, H. Minoura, Mechanism of cathodic electrodeposition of zinc oxide thin films from aqueous zinc nitrate baths, Thin Solid Films 451-452 (2004) 166-169.

[56] W. Yang, Z. Gao, J. Ma, J. Wang, X. Zhang, L. Liu, Two-step electrodeposition construction of flower-on-sheet hierarchical cobalt hydroxide nano-forest for high-capacitance supercapacitors, Dalton Trans 42(44) (2013) 15706-15.

[57] A. Krittayavathananon, S. Duangdangchote, P. Pannopard, N. Chanlek, S. Sathyamoorthi, J. Limtrakul, M. Sawangphruk, Elucidating the unexpected electrocatalytic activity of nanoscale PdO layers on Pd electrocatalysts towards ethanol oxidation in a basic solution, Sustainable Energy & Fuels 4(3) (2020) 1118-1125.

[58] E.S. Lambers, C.N. Dykstal, J.M. Seo, J.E. Rowe, P.H. Holloway, Room-temerature oxidation of Ni(110) at low and atmospheric oxygen pressures, Oxidation of Metals 45(3) (1996) 301-321.

[59] D.S. Hall, D.J. Lockwood, C. Bock, B.R. MacDougall, Nickel hydroxides and related materials: a review of their structures, synthesis and properties, Proceedings of the Royal Society A: Mathematical, Physical and Engineering Sciences 471(2174) (2015) 20140792.

[60] A.P. Grosvenor, M.C. Biesinger, R.S.C. Smart, N.S. McIntyre, New interpretations of XPS spectra of nickel metal and oxides, Surf. Sci. 600(9) (2006) 1771-1779.

[61] L. Marchetti, F. Miserque, S. Perrin, M. Pijolat, XPS study of Ni- base alloys oxide films formed in primary conditions of pressurized water reactor, Surface and Interface Analysis 47(5) (2015) 632-642.

[62] A. Dutta, J. Datta, Energy efficient role of Ni/NiO in PdNi nano catalyst used in alkaline DEFC, Journal of Materials Chemistry A 2(9) (2014) 3237-3250.

[63] M.S.E. Houache, E. Cossar, S. Ntais, E.A. Baranova, Electrochemical modification of nickel surfaces for efficient glycerol electrooxidation, Journal of Power Sources 375 (2018) 310-319.

[64] A.P. Grosvenor, M.C. Biesinger, R.S.C. Smart, N.S.J.S.S. McIntyre, New interpretations of XPS spectra of nickel metal and oxides, 600(9) (2006) 1771-1779.

[65] C.E. Dubé, B. Workie, S.P. Kounaves, A. Robbat, M.L. Aksub, G. Davies, Electrodeposition of Metal Alloy and Mixed Oxide Films Using a Single- Precursor Tetranuclear Copper- Nickel Complex, Journal of The Electrochemical Society 142(10) (1995) 3357-3365.

[66] A.M. Venezia, R. Bertoncello, G. Deganello, X-ray photoelectron spectroscopy investigation of pumice-supported nickel catalysts, Surface and Interface Analysis 23(4) (1995) 239-247.

[67] J.C. de Jesús, J. Carrazza, P. Pereira, F. Zaera, Hydroxylation of NiO films: the effect of water and ion bombardment during the oxidation of nickel foils with O2 under vacuum, Surface science 397(1-3) (1998) 34-47.

[68] K. Kim, N. Winograd, X-ray photoelectron spectroscopic studies of nickel-oxygen surfaces using oxygen and argon ion-bombardment, Surface Science 43(2) (1974) 625-643.

[69] M. Zhang, Z. Yan, Q. Sun, J. Xie, J. Jing, Synthetic core–shell Ni@Pd nanoparticles supported on graphene and used as an advanced nanoelectrocatalyst for methanol oxidation, New Journal of Chemistry 36(12) (2012) 2533-2540.

[70] M.S. Hamdan, N. Nordin, S.F.M. Amir, Electrochemical Behaviour of Ni and Ni-PVC Electrodes for the Electroxidation of Ethanol, Sains Malaysiana 40(12) (2011) 1421-1427.

[71] L. Zhang, Bimetallic Nickel and Copper Supported Pt Catalyst for Ethanol Electro-Oxidation in Alkaline Solution, International Journal of Electrochemical Science (2018) 2164-2174.

[72] J. Garcia-Aguilar, M. Navlani-Garcia, A. Berenguer-Murcia, K. Mori, Y. Kuwahara, H. Yamashita, D. Cazorla-Amoros, Evolution of the PVP-Pd Surface Interaction in Nanoparticles through the Case Study of Formic Acid Decomposition, Langmuir 32(46) (2016) 12110-12118.

[73] W. Chen, Y. Zhang, X. Wei, Catalytic performances of PdNi/MWCNT for electrooxidations of methanol and ethanol in alkaline media, International Journal of Hydrogen Energy 40(2) (2015) 1154-1162.

[74] Y. Zhao, L. Zhan, J. Tian, S. Nie, Z. Ning, Enhanced electrocatalytic oxidation of methanol on Pd/polypyrrole–graphene in alkaline medium, Electrochimica Acta 56(5) (2011) 1967-1972.

[75] Y. Wang, T.S. Nguyen, X. Liu, X. Wang, Novel palladium–lead (Pd–Pb/C) bimetallic catalysts for electrooxidation of ethanol in alkaline media, Journal of Power Sources 195(9) (2010) 2619-2622.

[76] R.N. Singh, A. Singh, Anindita, Electrocatalytic activity of binary and ternary composite films of Pd, MWCNT and Ni, Part II: Methanol electrooxidation in 1M KOH, International Journal of Hydrogen Energy 34(4) (2009) 2052-2057.

[77] S.Y. Shen, T.S. Zhao, J.B. Xu, Y.S. Li, Synthesis of PdNi catalysts for the oxidation of ethanol in alkaline direct ethanol fuel cells, Journal of Power Sources 195(4) (2010) 1001-1006.

[78] P. Parthasarathy, A.V. Virkar, Electrochemical Ostwald ripening of Pt and Ag catalysts supported on carbon, Journal of Power Sources 234 (2013) 82-90.

[79] M. Jin, H. Liu, H. Zhang, Z. Xie, J. Liu, Y. Xia, Synthesis of Pd nanocrystals enclosed by {100} facets and with sizes <10 nm for application in CO oxidation, Nano Research 4(1) (2010) 83-91.

[80] Y. Feng, K. Zhang, B. Yan, S. Li, Y. Du, Hydrothermal Method Using DMF as a Reducing Agent for the Fabrication of PdAg Nanochain Catalysts towards Ethanol Electrooxidation, Catalysts 6(7) (2016) 103.